The Effects of Gramicidin on Electroporation of Lipid Bilayers

Gregory C. Troiano,* Kathleen J. Stebe,# Robert M. Raphael,* and Leslie Tung*
*Department of Biomedical Engineering, The Johns Hopkins University, Baltimore, Maryland 21205, and #Department of Chemical Engineering, The Johns Hopkins University, Baltimore, Maryland 21218 USA

ABSTRACT The effects of the channel-forming peptide gramicidin D (gD) on the conductance and electroporation thresholds of planar bilayer lipid membranes, made of the synthetic lipid 1-palmitoyl 2-oleoyl phosphatidylcholine (POPC), was studied. High-amplitude (~200–900 mV) rectangular voltage pulses of 15 ms duration were used to perturb the bilayers and monitor the transmembrane conductance. Electroporation voltage thresholds were found, and conductance was recorded before and after electroporation. Gramicidin was added to the system in peptide/lipid ratios of 1:10,000, 1:500, and 1:15. The addition of gD in a ratio of 1:10,000 had no effect on electroporation, but ratios of 1:500 and 1:15 significantly increased the thresholds by 16% ($p < 0.0001$) and 40% ($p < 0.0001$), respectively. Membrane conductance before electroporation was measurable only after the addition of gD and increased monotonically as the peptide/lipid ratio increased. The effect of gD on the membrane area expansivity modulus (K) was tested using giant unilamellar vesicles (GUVs). When gD was incorporated into the vesicles in a 1:15 ratio, K increased by 110%, consistent with the increase in thresholds predicted by an electromechanical model. These findings suggest that the presence of membrane proteins may affect the electroporation of lipid bilayers by changing their mechanical properties.

INTRODUCTION

Electroporation is a process by which cell membranes become highly permeable after exposure to a high electric field (Tsong, 1991). This cellular response has been attributed to the formation of "electropores" in the lipid domain of the membrane, and has been well-studied and characterized in artificial lipid bilayers (Chizmadzhev and Pastushenko, 1988). Some groups have investigated the effects of non-phospholipid membrane constituents on electroporation. Some of these molecules, such as cholesterol (Needham and Hochmuth, 1989) and poloxamer 188 (Sharma et al., 1996), make the membranes less prone to electroporation. Others, such as lysophosphatidylcholine (LPC) (Chernomordik et al., 1985) and the surfactant $C_{12}E_8$ (Troiano et al., 1998), make membranes more susceptible. Although there are studies on the effects of membrane proteins on electrofusion (Ohno-Shosaku and Okada, 1985; Rols and Teissie, 1989; Longo et al., 1997), few experimental studies have investigated the fundamental roles that membrane proteins may play in the electroporation of lipid membranes.

Since membrane proteins are a major component in biological membranes, a full understanding of electroporation must take into account changes induced in the membrane by the presence of proteins. Such changes may be caused by lipid-protein interactions (Woolf and Roux, 1994). These interactions could stabilize or destabilize the membrane, and the nature of the interaction may be changed if the proteins undergo electric field-induced changes (Chen and Lee, 1994; Rosemberg et al., 1994). Membrane proteins could also alter the electric field across the bilayer. Characterizing these changes in lipid membranes in controlled situations will lead to a greater understanding of biomembrane electroporation.

One study of the effects of membrane proteins on electroporation claimed a twofold increase in the electroporation threshold after the insertion of liver mitochondrial proteins that increased membrane conductance (Kozhomkulov et al., 1984). Other researchers have speculated that transmembrane proteins or peptides could pack along the edges of pores and deter their resealing, thus making membrane resealing more difficult (Chernomordik et al., 1987). Rols and Teissie (1989) suggested that proteins limit not only the resealing, but also the extension of the pores in the lipid domains of the membrane, so that electropore growth could be inhibited or their size could be limited. It has also been proposed that electroporation is not entirely limited to lipid domains, but may occur through membrane channels which could then be denatured by Joule heating and sometimes removed from the membrane (Tsong, 1991).

Alterations in bilayer composition can cause changes in the electroporation of lipid bilayers by introducing stabilizing or destabilizing interactions within the membrane. These interactions would result in changes in the mechanical properties of the membrane. Such mechanical properties are usually measured in vesicle systems, in studies unrelated to electroporation. For example, LPC has been shown to have destabilizing mechanical effects on membranes in a vesicle study (Zhelev, 1996), and to decrease membrane lifetimes under electroporating fields in a planar bilayer study (Chernomordik et al., 1985). At least one study links electroporation to the mechanical properties,

Received for publication 28 July 1998 and in final form 15 March 1999.

Address reprint requests to Dr. Leslie Tung, Department of Biomedical Engineering, The Johns Hopkins University, 720 Rutland Avenue, Baltimore, MD 21205. Tel.: 410-955-7453; Fax: 410-955-0549; E-mail: ltung@bme.jhu.edu.

Gregory C. Troiano's current address is Guilford Pharmaceuticals, 6611 Tributary St., Baltimore, MD 21224.

0006-3495/99/06/3150/08 $2.00

both theoretically and experimentally (Needham and Hochmuth, 1989). This study found that electroporation thresholds increase with membrane area expansivity moduli and lysis tensions.

Being easier than proteins to characterize and incorporate into bilayers, transmembrane peptides are often studied to model membrane proteins and channels. Gramicidin D (gD) is a mixture of linear pentadecapeptides isolated from *Bacillus brevis* (Hotchkiss et al., 1940). Gramicidin A is the major component (~70%), while the rest are closely related peptides (Deamer, 1987; Prosser et al., 1994). When incorporated into lipid bilayers, monomers of gD can form head-to-head dimers that span the bilayer and form cation-selective ion channels. These channels are normally active until the dimer dissociates into two gD monomers, and have served as useful tools in studying lipid-protein interactions and ion channel conductances (Neher et al., 1978).

The membranes used for our experiments were bilayer lipid membranes (BLMs) and giant unilamellar vesicles (GUVs) composed of a single lipid, 1-palmitoyl 2-oleoyl phosphatidylcholine (POPC), to avoid difficulties inherent with mixtures of lipids with regard to experimental reproducibility. POPC is a zwitterionic lipid, and is a common constituent in biological membranes (Garrett and Grisham, 1995). In solution, it prefers to exist in the bilayer state (Israelachvili, 1985) and can easily form BLMs and GUVs at room temperature.

The goal of this study was to incorporate a small, well-characterized peptide into a pure lipid system, and to record the consequent changes in susceptibility to electroporation. Specifically, the effects of the channel-forming peptide, gD, on the electroporation and other electrical and mechanical properties of a pure POPC lipid bilayer, were investigated. The electroporation threshold and transmembrane conductance were found to be functions of gD concentration. The membrane area expansivity modulus of the bilayers was also found in unilamellar POPC vesicles to increase in the presence of gD.

MATERIALS AND METHODS

The lipid POPC was obtained in powder form (Avanti Polar Lipids; Alabaster, AL), from which either the bilayer-forming solution of 10 mg/ml in a 9:1 mixture of hexane and ethanol was made, or the vesicle-forming solution of 0.5 mg/ml in a 2:1 mixture of chloroform and methanol was made. Gramicidin D [Dubos] was also obtained in powder form (Sigma Chemical Company; St. Louis, MO), and dissolved in 200 proof ethanol. Deionized water, filtered to remove organic impurities, with a resistivity of 18 MΩ · cm, was used to make all solutions and in all cleaning procedures.

BLM experiments

Planar BLMs were formed by the folding method (Finkelstein, 1974) across a circular hole 105 μm in diameter in a 25-μm-thick Teflon sheet. The experimental setup and protocol to form bilayers in the Teflon bilayer chamber were similar to those used previously (Sharma et al., 1996; Troiano et al., 1998). Control experiments characterizing the electroporation thresholds and conductances of pure POPC bilayers were performed before every experiment with gD. For control, each compartment was filled with ~1.5 ml of a salt solution (100 mM KCl, 10 mM Hepes, pH 7.40), and POPC was deposited on the air-aqueous interface. After control was established, 15 μl gD in ethanol was injected just below the lipid layer into both compartments of the chamber before forming bilayers. Additions of similar amounts of ethanol alone had no effects on the electrical properties of the BLMs. The concentration of the injected solution was 100 times more concentrated than the final concentration in the 1.5-ml compartments. This final concentration is reported as a molar ratio of gD monomers in solution to the moles of lipid deposited at the air-aqueous interface ($2.64 \cdot 10^{-5}$ moles). Note that this may not reflect the ratio in the bilayer itself (see Discussion). The three ratios used in this study were 1:15, 1:500, and 1:10,000.

The membrane capacitance (C_m) and stray capacitance of the circuitry, chamber, and sheet were measured from charge pulse traces as previously described (Sharma et al., 1996). The system was pulsed for 10 μs at an intensity below the electroporation threshold, usually 300 mV or less. Specific capacitance (C_{sp}) was estimated for control membranes by dividing C_m by the membrane surface area (A_m), $7.79 \cdot 10^{-5}$ cm^2. The membrane was assumed to span 90% of the area of the hole ($8.66 \cdot 10^{-5}$ cm^2), with the remaining 10% of the hole area occupied by the torus of solvent that supports the membrane. C_{sp} was not measured for bilayers containing gD. At the sampling rate used in our system, it was not possible to accurately extract a time constant.

A 15-ms rectangular voltage pulse was used to perturb the membranes. The amplitude of the pulse (V_p) was varied systematically from a subthreshold level (50–250 mV) to the electroporation threshold of the membranes. For control membranes, the high resistance of the lipid bilayer assured that the potential across the membrane (V_m) was equal to V_p, and, after the membrane was stable for at least 5 min, V_m was incremented in steps of ~5 mV until electroporation took place. Pulses were separated by at least 15 s to allow the bilayer to have sufficient time to recover from the influence of previous pulses. The voltage that caused electroporation was recorded as the electroporation threshold of that membrane. Electroporation was irreversible, causing the membrane to rupture and the total conductance ($G_t = I_m/V_p$, where I_m is the current measured across the membrane) to rise until it reached that of a membrane-free state. This conductance included both the hole and the membrane conductances. The conductance of the bare hole (G_h) was recorded by applying a voltage pulse after membrane rupture. All experiments were performed at room temperature (22–24°C).

After gD injection, G_t increased. The effective membrane conductance (G_m) was calculated from the conductances with (G_t) and without (G_h) the membrane present. G_m increased with time after bilayer formation until a steady-state value was reached some 10–20 min later. After this steady-state value was attained, V_p was then incremented in steps of 5–50 mV until electroporation took place. Pulses were again separated by at least 15 s. The electroporation threshold was assumed to be the maximum value of transmembrane potential, V_m, calculated from V_p, G_h, and G_m, when the membrane ruptured (see Appendix).

Vesicle experiments

GUVs were prepared by rehydration under an external AC electric field (Angelova et al., 1992). Two 1-mm-diameter platinum electrodes, spaced 4 mm apart in a Teflon chamber (Fig. 1) were coated with 20 μl of the vesicle-forming solution and dried for 2 h under a vacuum. The chamber was then filled with an 80 mM sucrose solution.

The formation of vesicles was viewed under an inverted light microscope (Nikon Diaphot; Tokyo, Japan) at both 20× magnification and 40× magnification using Hoffman Modulation Contrast optics (Modulation Optics; Greenvale, NY). A sinusoidal, 10 Hz, AC voltage was applied across the electrodes and progressively increased from 0 to 2 V over 40 min. After 1 h the voltage was slowly decreased to 0.5 V while the frequency was decreased to 1 Hz. The vesicles, which had diameters of 10–100 μm, stopped growing after 2 h and detached from the electrodes after 4–5 h. They were stored under nitrogen at 4°C and diluted 1:1 with

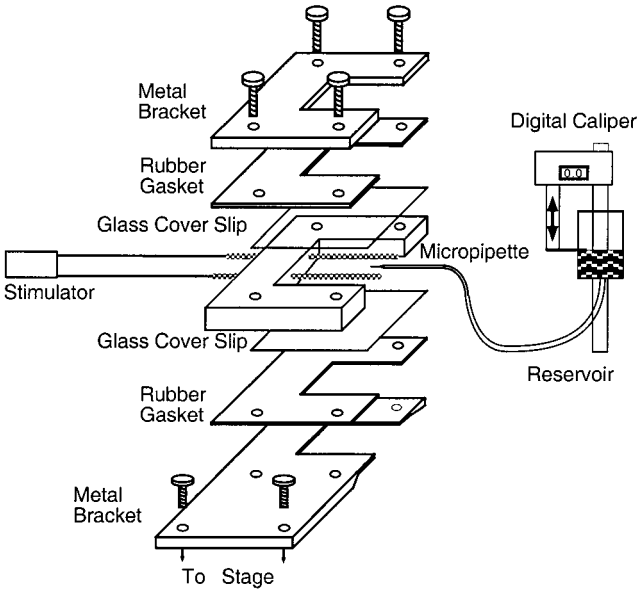

FIGURE 1 Schematic of the vesicle chamber. Vesicles were formed on the electrodes (*gray*). Vesicles were aspirated with micropipettes coupled to the reservoir, whose height was adjustable and monitored by a digital caliper.

a 90 mM glucose and/or sucrose solution in the vesicle chamber before experiments.

Pipettes were pulled from 1-mm capillary glass tubes to a fine point, and broken by quick fracture on a platinum microforge. The tips were broken to have a flat surface with inner diameters of 8–10 μm. The pipettes were filled with a solution containing 90 mM glucose and 0.3 wt/vol% BSA. The pipettes were then mounted on a micromanipulator and inserted into the chamber. Hydrostatic pressure was applied by a water-filled reservoir accurate to 0.1 mm H_2O as measured by a digital caliper (Starrett; Athol, MA). Zero pressure was found and checked frequently by observing that small ($\sim$1 μm) particles did not flow into or out of the pipette. Those vesicles that were selected had a thin wall, indicating that they were unilamellar, and possessed extra membrane area, so that they would produce long projections. They were aspirated into the micropipettes at low membrane tension, leaving an external spherical outer portion (Fig. 2). As the height of the reservoir was decreased, the pressure in the pipette (P_p) decreased. Since the pressure in the chamber (P_o) was constant, $P_o - P_p$ increased, and the projection length (L) increased. The membrane area expansivity moduli (K) were calculated from the slope of the change in membrane tension, τ, versus the change in membrane surface area, α (Evans and Rawicz, 1990). Assuming constant volume for the vesicle, α and τ can be calculated from the change in projection length (ΔL) and change in pressure ($\Delta P = P_o - P_p$), according to the following equations (Evans and Kwok, 1982):

$$\alpha = \frac{\Delta A}{A} \approx \frac{2\pi R_p \Delta L\left(1 - \frac{R_p}{R_{vo}}\right)}{4\pi R_v^2 - \pi R_p^2 + 2\pi R_p L} \quad (1)$$

$$\tau = \frac{\Delta P R_p}{2\left(1 - \frac{R_p}{R_v}\right)} \quad (2)$$

where R_p is the radius of the pipette, R_v the radius of the vesicle, and R_{vo} the initial radius (at very low ΔP). The region of low membrane tensions dominated by thermal fluctuations (Evans and Rawicz, 1990) was not investigated. After control was established, gD was injected into the chamber such that a 1:15 peptide/lipid ratio was achieved.

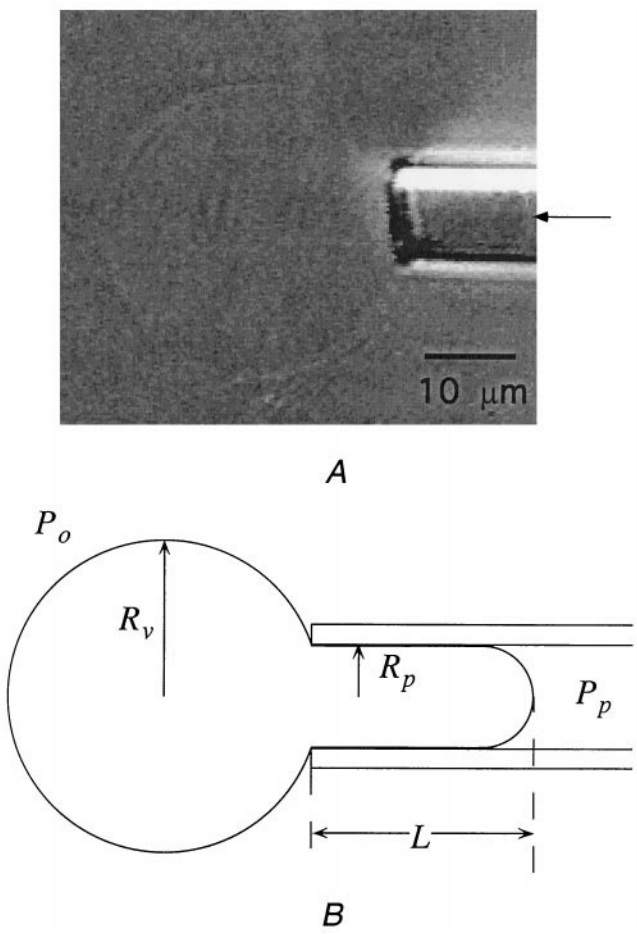

FIGURE 2 Aspirated vesicle, with parameters. (*A*) Image of a typical aspirated vesicle used in vesicle experiments. The arrow points to the vesicle projection. (*B*) Schematic of an aspirated vesicle. R_v is the radius of the vesicle, R_p the radius of the pipette, P_p the pressure in the pipette, P_o the pressure in the bath, and L the projection length.

Statistical analysis

The statistical significance of changes in parameters after changing peptide/lipid ratios was determined using pooled Student's *t*-tests. Values of $p < 0.05$ were considered significant for rejection of the null hypothesis.

RESULTS

The specific capacitance of control membranes was measured to be 0.60 $\pm$ 0.11 μF/cm^2 (n = 22). This value was similar to that found previously (Troiano et al., 1998) and in the range of values expected for artificial BLMs (Chizmadzhev and Pastushenko, 1988).

Typical current traces of a subthreshold voltage pulse for a control membrane (Fig. 3 *A*) and a membrane containing gD (Fig. 3 *B*) differed significantly. While control membranes had very high resistance and negligible G_m, membranes with gD contained ion-permeant channels that gave

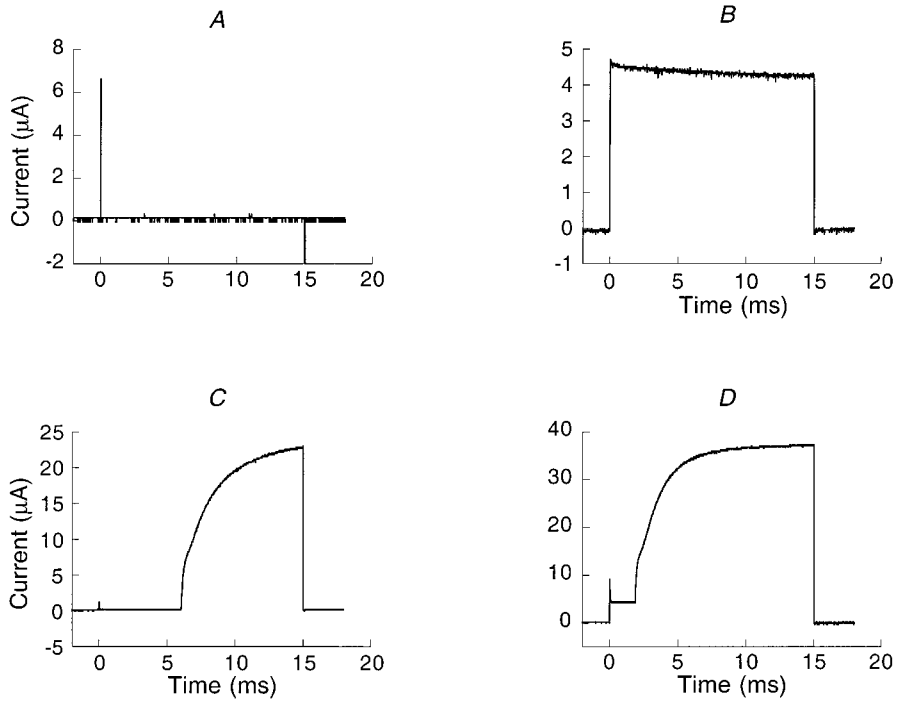

FIGURE 3 Typical current traces of membranes subjected to 15-ms duration voltage pulses. (*A*) A control membrane subjected to a subthreshold pulse 278 mV in amplitude. There was no current except for the two capacitive spikes at the onset and offset of the pulse. (*B*) A membrane with gD (1:500 peptide/lipid ratio) subjected to a subthreshold pulse 307 mV in amplitude ($\hat{V}_m$ = 270 mV). Because the membrane conductance was elevated by gD (~15 μS for this membrane), there was a current during the duration of the pulse, and $V_m \neq V_p$ (see Appendix). In most membranes this current decayed slightly with time (as shown here). (*C*) A control membrane subjected to a pulse 282 mV in amplitude, which elicits electroporation (at 6.06 ms), and a rise in current as the membrane ruptures. (*D*) A membrane with gD (1:500 peptide/lipid ratio) subjected to a pulse 370 mV in amplitude ($\hat{V}_m$ = 327 mV), which elicits electroporation (at 1.88 ms) and a current rise afterward that is caused by the increase in conductance as the membrane ruptures.

rise to a significant baseline current and G_m. When a pulse was of high enough amplitude and long enough duration to elicit electroporation, the current trace rose toward that of a membrane-free state for both control membranes (Fig. 3 *C*) and membranes with gD (Fig. 3 *D*). This current rise indicated the increase in conductance as the membrane ruptured.

Table 1 shows the electroporation thresholds for 15-ms pulses for control membranes and membranes with all three concentrations of gramicidin. Thresholds increased significantly from control when peptide/lipid ratios were 1:500 and increased even more for 1:15 ratios (Fig. 4).

Table 2 shows G_m for each of the gD concentrations used. The conductance of the bare hole (G_h) was measured to be 100 ± 10 μS/cm^2. Transmembrane conductance for control membranes was negligible (<0.5 μS) until electroporation, and was therefore reported as zero. As the concentration of gD increased, G_m increased monotonically. The current-voltage relationship of gD-treated membranes was linear over the entire range of voltages tested (from as low as 50 mV to the threshold). For membranes with large conductance, i.e., 1:500 and 1:15 ratios, G_m often decreased slightly over the duration of the pulse (Fig. 3 *B*). In these cases, the conductance just before the onset of electroporation was reported as G_m.

Fig. 5 shows typical graphs of membrane tension (τ) versus fractional area changes (α), calculated as described in the Methods section. Membrane area expansivity modulus (K), the slope of τ versus α on the graph, was found for pure POPC vesicles to be 227 ± 47 mN/m (n = 19). Lysis tensions for these vesicles were 11 ± 2.9 mN/m, with corresponding fractional surface area changes of 0.041 ± 0.011. The addition of gD to the vesicle bath (n = 4) increased K to 476 ± 149 mN/m ($p \leq 0.0001$) and the lysis tension to 25 ± 9 mN/m ($p \leq 0.0001$). The fractional surface area change at the new lysis tension was statistically unchanged from control values.

TABLE 1 Electroporation voltage thresholds for membranes with gD

Peptide/Lipid Ratio	Electroporation Threshold (mV)
Control (1:∞)	281 ± 31 (n = 22)
1:10,000	281 ± 27 (20)
1:500	327 ± 45 (20)*
1:15	393 ± 58 (10)*

Electroporation thresholds for membranes subjected to 15-ms pulses. Gramicidin concentration are given in peptide/lipid ratio. Thresholds for membranes with gD were compared to thresholds for control membranes using Student's t-tests. Those labeled with an asterisk (*) were statistically different from control ($p < 0.0001$). The number of bilayers tested is denoted by n.

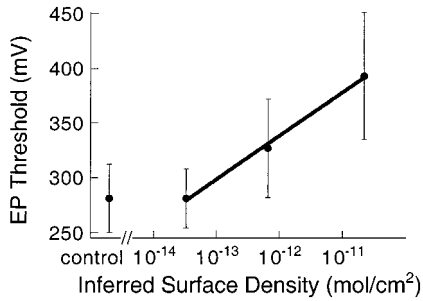

FIGURE 4 The electroporation thresholds of all membranes, plotted versus normalized gD concentration. The curve is the best semi-logarithmic fit for the data (R = 0.999). Inferred surface density is the theoretical surface density of gD based on the peptide/lipid ratios used (1:10,000, 1:500, and 1:15).

TABLE 2 Membrane conductances

Peptide/Lipid Ratio	G_m (μS)
Control (1:∞)	0 (n = 22)
1:10,000	1.611 ± .617 (20)
1:500	15.2 ± 10.2 (20)
1:15	106 ± 33 (10)

Baseline conductance (G_m), measured just before the onset of electroporation, is reported for each gD concentration. G_m for all peptide/lipid ratios were statistically compared using Student's t-tests. All data were statistically different from each other ($p < 0.0001$). The number of bilayers tested is denoted by n.

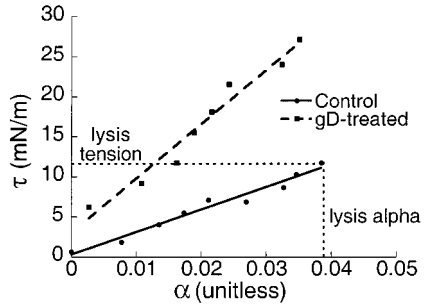

FIGURE 5 Membrane area expansivity moduli. These moduli (K) were computed by the slope of the best linear fit of τ versus α. Here, the graph of τ versus α after the addition of gD (*top, dashed line*) is compared to that of a control vesicle. K was 280 mN/m for the control vesicle (R = 0.984), and 676 mN/m for the gD-treated vesicle (R = 0.981). Lysis tension and lysis α occur at the uppermost data point, and are shown for the control membrane. Similar measurements were made for the gD-treated vesicle.

DISCUSSION

This study is, to our knowledge, the first quantitative analysis of the increase in electroporation thresholds after the incorporation of peptides into lipid membranes. The peptide gD was found to significantly increase the conductance and increase the electroporation voltage threshold of artificial POPC lipid bilayers, with all changes increasing monotonically with concentration. Pure POPC bilayers electroporated at a mean voltage of 281 mV for the 15-ms pulse durations used. This threshold increased to 327 mV and 393 mV for the two highest concentrations of gD tested (1:500 and 1:15 peptide/lipid ratios, respectively). Baseline G_m, which for control bilayers was negligible (<0.5 μS), also increased with increasing gD concentration. This conductance was 1.61 μS, 15.2 μS, and 106 μS for the 1:10,000, 1:500, and 1:15 ratios, respectively. GUVs were also used to measure the changes in bilayer area expansivity modulus, which also increased with gD incorporation.

Increases in electroporation threshold

Increases in the electroporation threshold with gD indicate a change in the response of the membrane to high electric fields. This could be caused by the formation of ion conducting channels and/or by a change in the mechanical properties of the bilayer. We do not believe that the higher electroporation threshold in gD membranes is related to increases in membrane conductivity for several reasons. Although the continuum theory of Maldarelli and Stebe (1992) predicts that an increase in conductivity may increase the electroporation threshold, the required conductivity increase for this effect is several orders of magnitude higher than was observed experimentally. Secondly, it can be argued that discrete aqueous pathways through a membrane may shunt the charge buildup across the membrane caused by the external electric field. If these pathways or channels are large enough, their shunting effect could act to decrease the effective transmembrane potential in the vicinity of the channel. This situation has been analyzed indirectly in the context of the access resistance to a pore (Hall, 1975) and the current distribution beneath a circular electrode (Wiley and Webster, 1982), and is described in the Appendix. Assuming a pore radius of 2 Å, pore conductance of 15 pS, and resistivity of solution of 67 Ω-cm, we estimate that the transmembrane potential at the mouth of the pore is reduced by ~2.5% from $\hat{V}_m$, but this reduction diminishes to 0.1% at only ~30 Å away from the center of the pore. Thus, the shunting effect is unlikely to explain the observed rise in threshold. Hence, both continuum and single-channel considerations suggest that increases in electroporation thresholds are not a result of the increase in membrane conductivity.

More likely reasons for the decrease in membrane susceptibility to electroporation are stabilizing lipid-monomer and lipid-dimer interactions. Stabilizing lipid-dimer interactions have been found in molecular dynamics simulations, particularly between the tryptophan side chains of the gD and the surrounding lipids (Woolf and Roux, 1994). Such interactions may cause gD to alter the mechanical properties of the membrane, and this was tested on GUVs in the present study. Such vesicles are also a well-characterized system, and have been used to evaluate the effects of various membrane constituents on their mechanical properties (Evans and Needham, 1986). Being primarily hydrophobic and incorporating into the fatty acid region of the bilayer, gD was shown in the present study to have effects similar to cholesterol, which increases both the area expansivity modulus and electroporation threshold of the membrane (Needham and Nunn, 1990; Evans and Needham, 1986; Needham and Hochmuth, 1989). The gD-induced increases of both K and lysis tension (Fig. 5) indicate an increase in the mechanical stability of the POPC membrane.

A number of electroporation models predict that increases in the mechanical stability of the membrane will increase membrane electroporation thresholds (Maldarelli and Stebe, 1992; Dimitrov, 1984; Needham and Hochmuth, 1989). In particular, the electromechanical model of Needham and Hochmuth (1989) predicts a relationship between area expansivity modulus and the electroporation threshold at zero membrane tension that takes the form

$$\frac{1}{2}\epsilon\epsilon_o\left(\frac{V_c}{h_e}\right)^2 h = K\alpha_c . \quad (3)$$

In Eq. 3, ϵ is the relative membrane dielectric constant ($\sim$2.2), ϵ_o the permittivity of free space, h_e the headgroup thickness, h the membrane thickness, and α_c the fractional surface area change at the lysis tension. For 1:15 gD GUVs, K was observed to increase by 110%, while α_c was not altered from control. Using these values in Eq. 3, a 45% increase in electroporation threshold is predicted. This increase agrees well with the 40% increase that was observed for the 1:15 gD BLMs experimentally. The 5% discrepancy may be attributed to experimental variability, but may also indicate that the inherent membrane tension in BLM systems is not entirely negligible.

It should be noted that the effects of gD on the mechanical properties of the membrane are in contrast with those effects found previously for very simple peptides, e.g., leucine residues with lysine terminals (Evans and Needham, 1987). These peptides have been shown to decrease the area expansivity modulus and lysis tension of vesicles, but are much different from gD, particularly in lacking hydrophilic tryptophans, which for gD dimers have stabilizing interactions with PC lipids (Woolf and Roux, 1994).

Dimerization of gD and membrane conductance

Injection of gD into the aqueous phase around lipid bilayers is expected to increase the conductance of the bilayers. The level of conductance achieved depends on at least four factors: how much gD is incorporated into the bilayer, how much gD dimerizes into channels, the type and ionic strength of the salt solution, and the transmembrane potential. The first two factors depend strongly on the concentration of gD (Neher et al., 1978), the constituents of the bilayer (Neher and Stevens, 1977; Girshman et al., 1997), the thickness of the bilayer (Veatch et al., 1975) and the temperature (Bamberg and Lauger, 1974). The amount that dimerizes can also depend on the transmembrane potential (Neher et al., 1978; Bamberg and Lauger, 1973). The last two factors affect the conductance of a single dimer channel (Andersen, 1983). Single channel conductances for gD in POPC bilayers surrounded by 100 mM KCl are expected to be $\sim$10–15 pS (Neher et al., 1978; Girshman et al., 1997). The mean lifetime of these channels is $\sim$0.5 s before they dissociate into two gD monomers (Girshman et al., 1997; Bamberg and Lauger, 1973).

Because there is an overabundance of lipid and gD, there may be a discrepancy between the peptide/lipid ratio deposited in the chamber and the peptide/lipid ratio actually in the bilayers. Only a small portion of the deposited lipid is in the bilayer. How much gD will be present in the bilayers compared to how much was added to the system is not easily determined, but was estimated and reported in Table 3. The estimates were obtained by using the experimentally measured conductance and a mass-action model for gD dimerization (Veatch et al., 1975), with a range of reported gD dimerization equilibrium constants (K_d) (Veatch et al., 1975; Bamberg and Lauger, 1973), and a POPC surface area of 0.5 nm^2/molecule.

TABLE 3 Gramicidin surface concentrations

Peptide/Lipid	Γ_2	Lowest Calculated Ratio	Highest Calculated Ratio
1:10,000	3.43	1:91,800	1:56
1:500	32.4	1:10,100	1:17
1:15	226	1:1460	1:6.0

Surface concentrations ($\cdot 10^{-15}$ mol/cm^2) of gD dimers (Γ_2), based on experimental conductance measurements, A_m, and a single channel conductance of 10 pS, are given for each concentration used. Lowest possible ratios and highest possible ratios correspond to the peptide/lipid ratios in the bilayers found after backing out Γ_0 from Γ_2, using K_d to be 10^{17} and 10^8 cm^2/mol, respectively.

CONCLUSIONS

Artificial bilayers have served as models for cell membranes to study the properties and kinetics of electroporation (Tsong, 1991). While they have been useful in the characterization of the process and underlying mechanisms, such bilayers are highly simplified models of a complex system. Cellular membranes consist of a myriad of membrane proteins, many of which respond to electric fields. The overall response of such a membrane to an electric field cannot be modeled without a consideration of these components. Analyzing the changes in electroporation parameters after adding biologically relevant molecules in a controlled manner is a step toward making artificial bilayers more realistic models for the cell membrane. The results of the planar BLM portion of this study indicate that the electroporation thresholds of lipid membranes increase in the presence of gD. The results of the vesicle experiments suggest that the increases in electroporation thresholds strongly correlate with an increase in the mechanical stability of the bilayers. These observations may be related to the observation of higher electroporation thresholds for cells than for pure lipid membranes (Abidor et al., 1979).

APPENDIX

Determination of V_m and G_m

Stimulus pulses (with amplitude V_p) were applied across the two compartments of the Teflon chamber, which were separated by a 105-μm hole in a 25-μm-thick Teflon sheet. For control membranes the membrane conductance is negligible, so that the transmembrane potential V_m is equal to the applied pulse potential V_p. For membranes with gD, however, V_m is only a fraction of V_p. Indeed, because of shunting by the gD pore, V_m will vary from a minimum of V_o at the mouth of the pore to a maximum of $\hat{V}_m$ well away from the pore. Far from the pore,

$$\hat{V}_m = \frac{R_g + 2R_a}{R_g + 2R_a + R_h + 2R_c} V_p \qquad \text{(A1)}$$

$$= \frac{1}{G_m R_t} V_p$$

where R_g is the aggregate resistance of the gD pores, R_a the aggregate access resistance (also referred to as spreading or convergence resistance) to one side of the pore, R_h the resistance of the hole through the Teflon

sheet, and R_c the resistance of one of the compartments of the chamber. The membrane conductance that we measure (G_m) is the reciprocal of the sum of pore and access resistances, i.e., $G_m = 1/(R_g + 2R_a)$. Two resistance measurements were made, one (R_b) in the absence (i.e., bare hole) and the other (R_t) in the presence of the gD-containing membrane:

$$R_b = R_h + 2R_c, \tag{A2}$$

$$R_t = R_g + 2R_a + R_h + 2R_c, \tag{A3}$$

The typical lengths and cross-sectional areas of the hole in the Teflon sheet and of the chamber ($l_h = 2.5 \cdot 10^{-3}$ cm, $A_h = 8.66 \cdot 10^{-5}$ cm^2, $l_c = 0.5$ cm, and $A_c = 1.8$ cm^2) were such that $R_c \ll R_h$ and therefore, $R_b \approx R_h$. R_h did not change between the two measurements, since the thickness of the bilayer ($\sim$10 nm) $\ll$ the hole thickness ($\sim$25 μm). Combining Eqs. A1–A3 together with the measured values for R_b and R_t yields estimated values of $\hat{V}_m = 0.98\ V_p$, $0.88\ V_p$, and $0.5\ V_p$ for 1:10,000, 1:500, and 1:15 gD/lipid bilayers, respectively.

At the mouth of the pore,

$$V_o = \frac{R_g}{R_g + 2R_a}\,\hat{V}_m. \tag{A4}$$

The ratio (R_g/R_a) was determined to be $\sim$80 from the ratio of access conductance for a single pore (Hall, 1975),

$$g_a = \frac{4a}{\rho} \tag{A5}$$

(where ρ is the resistivity of the medium, 67 Ω-cm) to the conductance of a single gD pore (assumed to be $\sim$15 pS). Combining Eqs. A4 and A5 together gives $V_o = 0.975\ \hat{V}_m$.

However, the effect of the gD shunt diminishes rapidly with distance from the hole. Adapting the results of Wiley and Webster (1982) for the case of a circular electrode placed on the surface of a semi-infinite volume conductor, to the case here of a circular pore within a nonconducting membrane with a potential V_o at its entrance,

$$V_m(r) = \begin{cases} V_o, & r \le a \\ \hat{V}_m - \left(\dfrac{2}{\pi}\sin^{-1}\dfrac{a}{r}\right)(\hat{V}_m - V_o), & r > a. \end{cases} \tag{A6}$$

where V_m is the transmembrane potential, a the pore radius, r the radial distance along the membrane from the center of the pore, and $\hat{V}_m$ the transmembrane potential far away from the pore. Note that Eq. A6 is only approximately correct for the case of the pore, since the equipotential surface at the entrance of the pore is not exactly a plane, as assumed in the derivation by Wiley and Webster.

At distances from the pore much larger than the pore radius but much smaller than the dimensions of the Teflon hole, the effects of the access resistance will have been exerted, and the potential in the bulk solution will be equal to $\hat{V}_m$. Thus, the shunting effect of the gD pore rapidly diminishes with increasing r, such that V_m rises from $\sim$97.5% $\hat{V}_m$ at the mouth of the pore to 99.9% $\hat{V}_m$ at $\sim$30 Å from the center of the pore.

The authors acknowledge the Whiting School of Engineering for funding the project and Thomas Woolf and John van Zanten for useful discussions.

REFERENCES

Abidor, I. G., V. B. Arakelyan, L. V. Chernomordik, Y. A. Chizmadzhev, V. F. Pastushenko, and M. R. Tarasevich. 1979. Electric breakdown of bilayer lipid membranes I. The main experimental facts and their qualitative discussion. *Bioelectrochem. Bioenerg.* 6:37–52.

Andersen, O. S. 1983. Ion movement through gramicidin A channels. Single-channel measurements at very high potentials. *Biophys J.* 41: 119–133.

Angelova, M. I., S. Soleau, P. Meleard, J. F. Faucon, and P. Bothorel. 1992. Preparation of giant vesicles by external AC electric fields. Kinetics and applications. *Prog. Colloid Polym. Sci.* 89:127–131.

Bamberg, E., and P. Lauger. 1973. Channel formation kinetics of gramicidin A in lipid bilayer membranes. *J. Membr. Biol.* 11:177–194.

Bamberg, E., and P. Lauger. 1974. Temperature-dependent properties of gramicidin A channels. *Biochim. Biophys. Acta.* 367:127–133.

Chen, W., and R. C. Lee. 1994. Altered ion channel conductance and ionic selectivity induced by large imposed membrane potential pulse. *Biophys. J.* 67:603–612.

Chernomordik, L. V., M. M. Kozlov, G. B. Melikyan, I. G. Abidor, V. S. Markin, and Y. A. Chizmadzhev. 1985. The shape of lipid molecules and monolayer membrane fusion. *Biochim. Biophys. Acta.* 812:643–655.

Chernomordik, L. V., S. I. Sukharev, S. V. Popov, V. F. Pastushenko, A. V. Sokirko, I. G. Abidor, and Y. A. Chizmadzhev. 1987. The electrical breakdown of cell and lipid membranes: the similarity of phenomenologies. *Biochim. Biophys. Acta.* 902:360–373.

Chizmadzhev, Y. A., and V. F. Pastushenko. 1988. Electrical breakdown of bilayer lipid membranes. *In* Thin Liquid Films. Marcel Dekker, New York. 1059–1120.

Deamer, D. W. 1987. Proton permeation of lipid bilayers. *J. Bioenerg. Biomembr.* 19:457–479.

Dimitrov, D. S. 1984. Electric field-induced breakdown of lipid bilayers and cell membranes: a thin viscoelastic film model. *J. Membr. Biol.* 78:53–60.

Evans, E., and R. Kwok. 1982. Mechanical calorimetry of large dimyristoylphosphatidylcholine vesicles in the phase transition region. *Biochemistry.* 21:4874–4879.

Evans, E., and D. Needham. 1986. Giant vesicle bilayers composed of mixtures of lipids, cholesterol and polypeptides. Thermomechanical and (mutual) adherence properties. *Faraday Discuss. Chem. Soc.* 81: 267–280.

Evans, E., and D. Needham. 1987. Physical properties of surfactant bilayer membranes: thermal transitions, elasticity, rigidity, cohesion, and colloidal interactions. *J. Phys. Chem.* 91:4219–4228.

Evans, E., and W. Rawicz. 1990. Entropy-driven tension and bending elasticity in condensed-fluid membranes. *Phys. Rev. Lett.* 64: 2094–2097.

Finkelstein, A. 1974. Bilayers: formation, measurements, and incorporation of components. *Methods Enzymol.* 32:489–501.

Garrett, R. H., and C. M. Grisham. 1995. Biochemistry. Saunders College Publishing and Harcourt Brace College Publishers, Fort Worth.

Girshman, J., D. Greathouse, R. Koeppe, and O. Andersen. 1997. Gramicidin channels in phospholipid bilayers with unsaturated acyl chains. *Biophys. J.* 73:1310–1319.

Hall, J. 1975. Access resistance of a small circular pore. *J. Gen. Phys.* 66:531–532.

Hotchkiss, R., D. Rollin, and R. Dubos. 1940. Fractionation of the bactericidal agent from cultures of a soil bacillus. *J. Biol. Chem.* 132: 791–792.

Israelachvili, J. N. 1985. Aggregation of amphiphilic molecules into micelles, bilayers, vesicles, and biological membranes. *In* Intermolecular and Surface Forces: With Applications to Colloidal and Biological Systems. Academic Press, London; Orlando. Chap. 17.

Kozhomkulov, E., K. Normatov, S. Azimova, and A. Marzoev. 1984. [Modification of the electric characteristics of bilayer lipid membranes by intramitochondrial thyroid hormone receptors]. *Probl. Endokrinol. (Mosk).* 30:60–63.

Longo, M. L., A. J. Waring, and D. A. Hammer. 1997. Interaction of the influenza hemagglutinin fusion peptide with lipid bilayers: area expansion and permeation. *Biophys. J.* 73:1430–1439.

Maldarelli, C., and K. Stebe. 1992. An anisotropic, elastomechanical instability theory for electropermeabilization of bilayer-lipid membranes. *In* Electrical Trauma: The Pathophysiology, Manifestations, and Clinical Management. R. C. Lee, E. G. Cravalho, and J. F. Burke, editors. University of Cambridge Press. 327–360.

Needham, D., and R. M. Hochmuth. 1989. Electromechanical permeabilization of lipid vesicles. Role of membrane tension and compressibility. *Biophys. J.* 55:1001–1009.

Needham, D., and R. S. Nunn. 1990. Elastic deformation and failure of lipid bilayer membranes containing cholesterol. *Biophys. J.* 58: 997–1009.

Neher, E., J. Sandblom, and G. Eisenman. 1978. Ionic selectivity, saturation, and block in gramicidin A channels. II. Saturation behavior of single channel conductances and evidence for the existence of multiple binding sites in the channel. *J. Membr. Biol.* 40:97–116.

Neher, E., and C. F. Stevens. 1977. Conductance fluctuations and ionic pores in membranes. *Annu. Rev. Biophys. Bioeng.* 6:345–381.

Ohno-Shosaku, T., and Y. Okada. 1985. Electric pulse-induced fusion of mouse lymphoma cells: roles of divalent cations and membrane lipid domains. *J. Membr. Biol.* 85:269–280.

Prosser, R. S., S. I. Daleman, and J. H. Davis. 1994. The structure of an integral membrane peptide: a deuterium NMR study of gramicidin. *Biophys. J.* 66:1415–1428.

Rols, M. P., and J. Teissie. 1989. Ionic-strength modulation of electrically induced permeabilization and associated fusion of mammalian cells. *Eur. J. Biochem.* 179:109–115.

Rosemberg, Y., M. Rotenberg, and R. Korenstein. 1994. Electroporation of the photosynthetic membrane: structural changes in protein and lipid-protein domains. *Biophys J.* 67:1060–1066.

Sharma, V., K. Stebe, J. C. Murphy, and L. Tung. 1996. Poloxamer 188 decreases susceptibility of artificial lipid membranes to electroporation. *Biophys. J.* 71:3229–3241.

Troiano, G., K. Stebe, V. Sharma, and L. Tung. 1998. The electroporation of artificial planar POPC bilayers and the effects of $C_{12}E_8$ on its properties. *Biophys. J.* 75:880–888.

Tsong, T. Y. 1991. Electroporation of cell membranes. *Biophys. J.* 60: 297–306.

Veatch, W., R. Mathies, M. Eisenberg, and L. Stryer. 1975. Simultaneous fluorescence and conductance studies of planar bilayer membranes containing a highly active and fluorescent analog of gramicidin A. *J. Mol. Biol.* 99:75–92.

Wiley, J. D., and J. G. Webster. 1982. Analysis and control of the current distribution under circular dispersive electrodes. *IEEE Trans. Biomed. Eng*. BME29:381–385.

Woolf, T. B., and B. Roux. 1994. Molecular dynamics simulation of the gramicidin channel in a phospholipid bilayer. *Proc. Natl. Acad. Sci. U.S.A.* 91:11631–11635.

Zhelev, D. V. 1996. Exchange of monooleoylphosphatidylcholine with single egg phosphatidylcholine vesicle membranes. *Biophys. J.* 71: 257–273.